

## A unified Raman picture from nano-crystalline graphite to amorphous carbons: electron-phonon coupling and aromatic domain size

Cedric Pardanaud, Celine Martin, Pascale Roubin

Lab. PIIM (UMR 6633 CNRS-Universite de Provence) Saint-Jerome, F-13397 Marseille Cedex 20  
[cedric.pardanaud@univ-provence.fr](mailto:cedric.pardanaud@univ-provence.fr)

Raman microspectroscopy is routinely used for characterizing carbons. Structural information can be obtained thanks to previous works by coupling with other techniques. The shape of the Raman spectra depends on the excitation wavelength and, from IR to near UV, is sensitive to the  $sp^2$  content of the material, the G and D band parameters being strongly dependent on their nanostructure. Raman analysis can give an estimation of how the material is disordered:  $sp^2/sp^3$  ratio, %H... can be estimated. We focus here on several Raman parameters: the G band wavenumber  $\sigma_G$ , the G and D band widths  $\Gamma_G$  and  $\Gamma_D$  together with their relative intensities  $R=H_D/H_G$ . We extend some properties known for nanocrystalline graphite to amorphous carbons, such as the Raman diffusion cross-section dependence with the excitation wavelength, and also some properties known for amorphous carbons to nanocrystalline graphite, such as the cluster size estimation ( $L_a$ ) using various excitation wavelengths. We also give evidence for the importance of the electron-phonon coupling on the D band width of a large range of disordered carbons.

To interpret Raman signals of a large variety of carbons (graphitic, nc-G, a-C:H, ...) we have investigated carbonaceous samples from the plasma facing components of the Tore Supra tokamak (referred as TS samples), both the virgin C/C composite and the carbon deposits formed during plasma operation. Figure 1-a displays typical Raman spectra obtained for these samples with  $\lambda_L=514.5$  nm. C/C samples are graphitic carbons. TS spectra are more heterogeneous: some are similar to a-C spectra with broad G and D bands while some either are similar to nc-G spectra with well separated G and D bands or look intermediate, between nc-G or a-C spectra. We have analyzed a great amount of data, focusing on relations between  $\sigma_G$ ,  $\Gamma_G$  and  $\Gamma_D$ , and the D and G band relative intensity, R, and we have emphasized the similarity of nc-G and a-C properties revealed by the continuous clouds formed by Raman parameters, as shown for example for  $\Gamma_G$  in figure 1.b.

Data, recorded with  $\lambda_L=325.0$ , 514.5 and 785.0 nm, have been interpreted in the framework of laws linking Raman parameters together known from the literature. For nano-crystalline samples, these laws are the Tuinstra relation [1] and the  $\lambda_L$  dependence of R [2]. These studies have also shown that  $\Gamma_G$  could be approximated for such materials by a linear law with R. For a-C data, we have used the relations proposed by Ferrari and Robertson [3,4] for R and  $\Gamma_G$  for the green excitation wavelength.

Then, we have assumed first, a similar fourth power  $\lambda_L$  dependency for a-C than for nc-G and second, continuity between nc-G and a-C at  $L_a = L_{a0}$ . With these simple assumptions, and defining the scaled intensity ratio  $R_\lambda = R \times (514.5/\lambda_L)^4$ , we succeed in fitting a-C data for the three  $\lambda_L$  used in this study. Figure 1.b displays experimental (points) and fitted (lines) Raman parameters in the  $(R_\lambda, \Gamma_G)$  plot in the case of  $\lambda_L=325$  nm (blue) and 514.5 nm (green) data. The good fit obtained indicates that the  $\lambda_L$  dependency of R is shared by both a-C and nc-G.

Nevertheless a lot of green data are still not reproduced using this modeling and we divide TS samples in three groups: pure nc-G, pure a-C, and intermediate samples, these latter samples being those not correctly described by the previous laws (grey lines of figure 1.b). We propose to interpret these spectra as the sum of two sets of bands: one nc-G set composed of three bands, G, D and D', and one a-C set composed of two bands, G and D. The ratio between these two sets of bands. This choice is supported by the spectral decomposition usually made in the literature [5, 7]. Our method thus consists in first building simulated spectra by adding these two sets of bands using realistic parameters (with the "s" exponent, meaning "simulation") and second analyzing these simulated spectra with their raw Raman parameters exactly in the same way as the experimental spectra. The curve of figure 1.b at low  $\Gamma_G$  ( $\Gamma_G < 80$   $cm^{-1}$ ), referred to as simulation S1, is obtained by only taking into account the nc-G set of bands. For larger  $\Gamma_G$ , a deviation from the grey line appears which qualitatively reproduces the experimental trend. This origin of the deviation from a straight line is thus merely the apparent broadening of the G band due to the presence of the D' band. To reproduce the experimental trends at larger  $\Gamma_G$ , introducing the a-C set of bands is needed, as shown with simulation S2. Finally, to correctly simulate spectra with  $\Gamma_G > 80$   $cm^{-1}$  an additional broadening  $\Gamma_{add}$  is needed for the G and D bands of nc-G, (simulation S3).

Figure 2 displays  $\Gamma_D$  versus  $\Gamma_G$  (experimental and simulated data). Graphitic and pure nc-G, intermediate and a-C sample widths have been displayed for the green excitation wavelength. C/C data points are localized on the straight line corresponding to  $\Gamma_D = 2 \Gamma_G$ . All the TS data points are distributed around this straight line, S-shaped. According to [8] the natural broadening of the G band for graphene is proportional to  $\langle D_{\Gamma^2} \rangle_F$  which is called the electron-phonon coupling at the  $\Gamma$  point of the Brillouin zone (EPC, see [9]). These authors have also shown that  $\langle D_{K^2} \rangle_F / \langle D_{\Gamma^2} \rangle_F = 2$  where  $\langle D_{K^2} \rangle_F$  is the electron phonon coupling at the K point of the Brillouin zone. As the phonons at this K point are involved in the existence of the D band of disordered carbons this is an indication that electron-phonon coupling plays a similar role for all types of carbon.

To conclude, we have shown that fundamental properties such as the  $\lambda_L$  dependency of the Raman cross-section and the electron-phonon induced broadening could be used to interpret nc-G as well as a-C data, indicating common trends and a continuum of properties among these types of carbons. We thus get a consistent description of the Raman properties of both types of carbon.

## References

- [1] F. Tuinstra, and J. L. Koenig, J. Chem. Phys. **53** (1970) 1126
- [2] L. G. Cançado, A. Jorio, and M. A. Pimenta, Phys. Rev. B **76** (2007) 064304
- [3] A. C. Ferrari, and J. Robertson, Phys. Rev. B **61** (2000) 14095
- [4] A. C. Ferrari, and J. Robertson, Phil. Trans. R. Soc. Lond. A **362** (2004) 2477
- [5] C. Beny-Bassez, and J. N. Rouzaud, Scanning electron microscopy **1** (1985) 119
- [6] T. Jawhari, A. Roid, and J. Casado, Carbon **33** (1995) 1561
- [7] A. Sadezky *et al.*, Carbon **43** (2005) 1731
- [8] S. Piscanec *et al.*, Phys. rev. lett. **93** (2004) 185503
- [9] M. Lazzeri *et al.*, Physical review B **73** (2006) 155426

## Figures

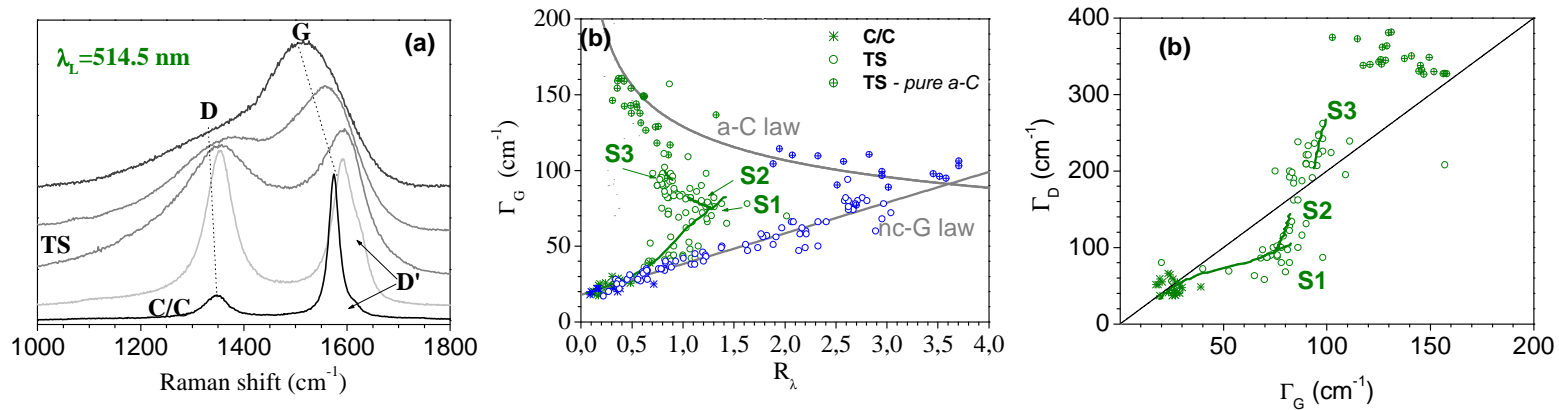


Figure 1. Raman data corresponding to C/C and Tore Supra samples (green for  $\lambda_L = 514.5$  nm, blue for  $\lambda_L = 325.0$  nm). (a) Typical Raman spectra of C/C and TS samples. (b) Raman parameters compared to simulations. Simulation S1 is obtained with a pure nc-G component. Simulation S2 is obtained by adding to a nc-G component an a-C component with the introduction of an additional broadening for S3 simulation. (c) is the same as (b) but in the  $(\Gamma_G, \Gamma_D)$  plot.